Control of the Restriction Point by Rb and p21

Justin Moser[a,b], Iain Miller[a,b], Dylan Carter[a,b], and Sabrina L. Spencer[a,b,1]

[a]Department of Biochemistry, University of Colorado–Boulder, Boulder, CO 80303; and [b]BioFrontiers Institute, University of Colorado–Boulder, Boulder, CO 80309

Edited by Tim Hunt, Cancer Research UK, London, United Kingdom, and approved July 10, 2018 (received for review December 27, 2017)

The Restriction Point was originally defined as the moment that cells commit to the cell cycle and was later suggested to coincide with hyperphosphorylation of the retinoblastoma protein (Rb). Current cell cycle models posit that cells exit mitosis into a pre-Restriction Point state, where they have low cyclin-dependent kinase (CDK) activity and hypophosphorylated Rb; passage through the Restriction Point then occurs in late G1. Recent single-cell studies have challenged the current paradigm, raising questions about the location of the Restriction Point and the notion that cells exit mitosis into a pre-Restriction Point state. Here, we use a variety of single-cell techniques to show that both noncancer and cancer cells bifurcate into two subpopulations after anaphase, marked by increasing vs. low CDK2 activity and hyper- vs. hypophosphorylation of Rb. Notably, subpopulations with hyper- and hypophosphorylated Rb are present within minutes after anaphase, delineating one subpopulation that never "uncrosses" the Restriction Point and continues cycling and another subpopulation that exits mitosis into an uncommitted pre-Restriction Point state. We further show that the CDK inhibitor p21 begins rising in G2 in mother cells whose daughters exit mitosis into the pre-Restriction Point, CDK2^{low} state. Furthermore, degradation of p21 coincides with escape from the CDK2^{low} state and passage through the Restriction Point. Together, these data support a model in which only a subset of cells returns to a pre-Restriction Point state after mitosis and where the Restriction Point is sensitive to not only mitogens, but also inherited DNA replication stress via p21.

cell cycle | restriction point | quiescence | G0 | CDK2

The ability of cells to transition between proliferative and quiescent states is critical for organismal health, as this enables tissue development and maintenance while preventing cancer (1). To commit to the cell cycle and proliferate, cells must cross the Restriction Point, after which they will complete the current cell cycle, even if serum or mitogens are withdrawn. Early serum withdrawal–restimulation–withdrawal experiments in synchronized cells suggested that cells arrest at a single point between mitosis and S phase until serum and mitogen conditions become favorable to proliferation once again (2). It was later shown that pulsed, rather than constant, mitogen exposure was sufficient to cross the Restriction Point and commit cells to a round of proliferation (3, 4). Similarly, time-lapse microscopy of asynchronously cycling Swiss 3T3 cells suggested that cycling cells are sensitive to serum withdrawal for only the first 3–4 h after mitosis, putting the Restriction Point in this interval (5). Based on these data, a model emerged that both cycling cells and cells emerging from serum starvation were subject to a mid- to late-G1 Restriction Point. Cells pre-Restriction Point are uncommitted to the cell cycle and can arrest at the Restriction Point, whereas cells post-Restriction Point are no longer dependent on mitogens and will complete one round of division, even in the absence of mitogens.

Molecular biological and biochemical investigations later uncovered the molecular and systems-level basis for the Restriction Point, with the retinoblastoma protein (Rb) and cyclin:cyclin-dependent kinase (CDK) complexes coming to the fore. Based on work in cells emerging from serum starvation, serum restimulation results in the buildup of cyclin D (6), which in complex with CDK4/6, initiates the process of Rb phosphorylation (7). In the canonical model, this liberates some E2F, which initiates transcription of cyclins E and A. These cyclins in complex with CDK2 help generate the positive feedback loop that triggers the switch from hypo- to hyperphosphorylated Rb (8), marking cell cycle commitment (9). This fully releases E2F and leads to the production of other genes critical for S-phase entry.

Based on work in cells synchronized in mitosis by nocodazole and subsequently released, the switch from hyperphosphorylated to hypophosphorylated Rb was shown to begin in late anaphase and continue through early G1 (10). The activity of CDKs, in particular CDK2, then triggers the switch from hypo- to hyperphosphorylated Rb at the Restriction Point and underlies the bistability of this system (7, 11, 12). Thus, activation of CDK2 and hyperphosphorylation of Rb indicate passage through the Restriction Point. The synthesis of these observations led to a model of the cell cycle in which cells are born into an uncommitted state characterized by low CDK activity and hypophosphorylated Rb (Fig. 1*A*) (13). On crossing the Restriction Point several hours after mitosis with the hyperphosphorylation of Rb, cells are committed to one round of the cell cycle, giving rise to two daughter cells again born into a state of low CDK activity and hypophosphorylated Rb.

Although this model of the cell cycle is widely accepted, recent studies in asynchronously cycling cells have challenged this paradigm. The development of a CDK2 activity sensor revealed two classes of cellular behavior after mitosis in the mammary epithelial cell line MCF10A (14). Some cells follow the expected paradigm, wherein after mitosis, CDK2 activity turns off, Rb becomes dephosphorylated, and cells are once

Significance

The canonical Restriction Point model suggests that cells are born into a state in which they are uncommitted to the cell cycle, but will activate cyclin-dependent kinase 2 and cross the Restriction Point several hours later if sufficient nutrients are available. However, recent single-cell studies have challenged aspects of this model. This work examines the Restriction Point in cancerous and noncancerous cells and shows that, in six cases tested, the cell populations split such that only a subset of cells is born into a pre-Restriction Point state, while the remainder immediately commits to another cell cycle. This shows that even cancer cells can experience significant heterogeneity in this cell fate decision, which may be exploitable for therapeutic gain.

Author contributions: J.M. designed research; J.M., I.M., and D.C. performed research; J.M. and S.L.S. analyzed data; S.L.S. conceived of the project; and J.M. and S.L.S. wrote the paper.

The authors declare no conflict of interest.

This article is a PNAS Direct Submission.

[1]To whom correspondence should be addressed. Email: sabrina.spencer@colorado.edu.

This article contains supporting information online at www.pnas.org/lookup/suppl/doi:10.1073/pnas.1722446115/-/DCSupplemental.

Published online August 15, 2018.

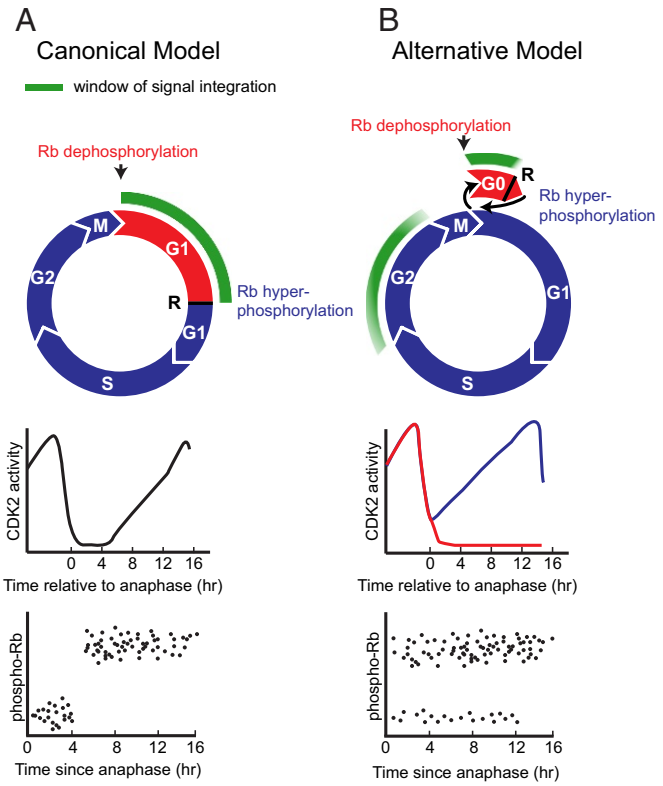

Fig. 1. Two models of the Restriction Point depicted using simulated data. (*A*) The canonical model of the cell cycle predicts that cells are born into a pre-Restriction Point state characterized by low CDK2 activity, hypophosphorylated Rb, mitogen sensitivity, and lack of cell cycle commitment. This state has been referred to variously as "early G1" and "$G1_{pm}$" (5, 7). Then, 3–4 h after mitosis, cells reach the Restriction Point (R). Given optimal conditions, cells cross the Restriction Point and become committed to the cell cycle. This state has been referred to as "late G1" and "$G1_{ps}$" (5, 7). (*B*) An alternative cell-cycle model that takes into account recent studies, in which cells integrate mitogen and stress signaling during a maternal window of signal integration that informs the G0–G1 decision that occurs after mitosis. One subpopulation is born with moderate CDK2 activity and hyperphosphorylated Rb, is insensitive to mitogen withdrawal, and is committed to the cell cycle, whereas the other subpopulation is born with low CDK2 activity and hypophosphorylated Rb and remains sensitive to mitogen withdrawal, similar to the cells diagrammed in *A*. The proliferative subpopulation thus never uncrosses the Restriction Point, whereas the $CDK2^{low}$ subpopulation is born into a pre-Restriction Point state that can be considered a transient G0. These cells emerge from the $CDK2^{low}$ state to reengage with the cell cycle by building up CDK2 activity and hyperphosphorylating Rb.

again mitogen sensitive ("$CDK2^{low}$ cells"). $CDK2^{low}$ cells are not senescent, and cells can remain in this state anywhere from a few hours to multiple days before reentering the cell cycle (15). While the $CDK2^{low}$ state could be conceptualized as "early G1," it also has many features consistent with a transient G0 or quiescence, including declining Ki67 protein levels (16), little to no CDK2 activity, hypophosphorylated Rb, and elevated p21 (14). In contrast, other cells show increasing CDK2 activity after mitosis, hyperphosphorylated Rb, and mitogen insensitivity, and they immediately commit to another cell cycle ("$CDK2^{inc}$ cells") (14). Moreover, the CDK2 activity sensor can be used to visualize passage through the Restriction Point: cells in the $CDK2^{low}$ state are mitogen sensitive and become locked in the $CDK2^{low}$ state if mitogens are withdrawn, but after cells build up CDK2 activity above a threshold level, they become mitogen insensitive and continue progression through the cell cycle, even if mitogens are withdrawn or the MAPK pathway is inhibited (14, 17, 18).

Recent papers suggest that entry into quiescence is facilitated during the maternal G2 (14, 19) and that spontaneous entry into the $CDK2^{low}$ state is caused in part by low-level endogenous DNA replication stress that is passed from mother cells to daughter cells (20–23). Furthermore, the CDK2 inhibitor, p21, was found to be up-regulated in these stressed cells and was required for entry into the $CDK2^{low}$ state after both endogenous and exogenous replication stress (20, 21). Thus, p21 seems to be a critical component of the Restriction Point decision, but its exact connection to the Restriction Point is unclear.

Based on these recent findings, we propose here that healthy cells in optimal growth conditions cycle continuously without ever "uncrossing" the Restriction Point or losing Rb phosphorylation (Fig. 1*B*), whereas the classic Restriction Point model predicts that cells are born into a pre-Restriction Point state with hypophosphorylated Rb and low CDK2 activity (Fig. 1*A*). Distinguishing between these two models and establishing their generalizability are necessary for improving our understanding of how cells behave both in cell culture and in vivo. The canonical model of the cell cycle ignores the behavioral heterogeneity as well as its underlying causes that have been unearthed in recent years. It thus incompletely acknowledges the various mechanisms and timing thereof that regulate cell cycle commitment, exit, and reentry.

In this manuscript, we show the applicability of the alternative model across five widely used transformed and nontransformed cell lines and one type of primary cell, all of which have functional Rb and p53, establishing its validity beyond MCF10A cells. We show that all of these cell lines display a bifurcation in CDK2 activity and Rb phosphorylation at mitotic exit. This result contrasts with the canonical cell cycle model, in which cells have hypophosphorylated Rb after anaphase. Furthermore, by tracking p21 under endogenous control in single cells over multiple cell cycles, we detect the up-regulation of p21 in G2 phase of mother cells whose daughters enter the $CDK2^{low}$ state after mitosis. We further show that these $CDK2^{low}$ cells reenter the cell cycle by degrading p21 at the Restriction Point. Together, these data reveal that only a fraction of cells in the cell types examined here display features of the canonical model and exit mitosis into a pre-Restriction Point state of hypophosphorylated Rb. Our results instead support an alternative model in which, under saturating mitogens, the proliferation–quiescence decision is influenced strongly by the G2/M levels of p21, which if high enough, result in the dephosphorylation of Rb in telophase, and the reset of those cells to a pre-Restriction Point state.

Results

A Bifurcation in CDK2 Activity and Rb Phosphorylation After Mitosis Is Present in both Transformed and Nontransformed Cell Types. The observation of a bifurcation in CDK2 activity after mitosis in unperturbed cells was initially made in nontransformed MCF10A mammary epithelial cells (14). To determine the generalizability of this finding, we examined several noncancerous (MCF10A and retinal RPE-hTERT) and cancerous (mammary MCF7, osteosarcoma U2OS, and colorectal HCT116) cells as well as primary human lung fibroblasts (HLFs). HLFs were recently reported to follow the canonical model depicted in Fig. 1*A* rather than the alternative model in Fig. 1*B* (17). We transduced all six cell types with fluorescent histone 2B (H2B) as a nuclear marker as well as the CDK2 activity sensor and monitored CDK2 activity by time-lapse imaging and cell tracking in asynchronously cycling cells. Despite the wide variety of cell types examined, each showed a bifurcation in CDK2 activity at mitotic exit (Fig. 2*A* and Movies S1–S6). Notably, the cancer lines did not always show a lower fraction of $CDK2^{low}$ cells than MCF10A. Only HCT116 cells, with 1% $CDK2^{low}$, were significantly more proliferative than MCF10A cells, with 26%

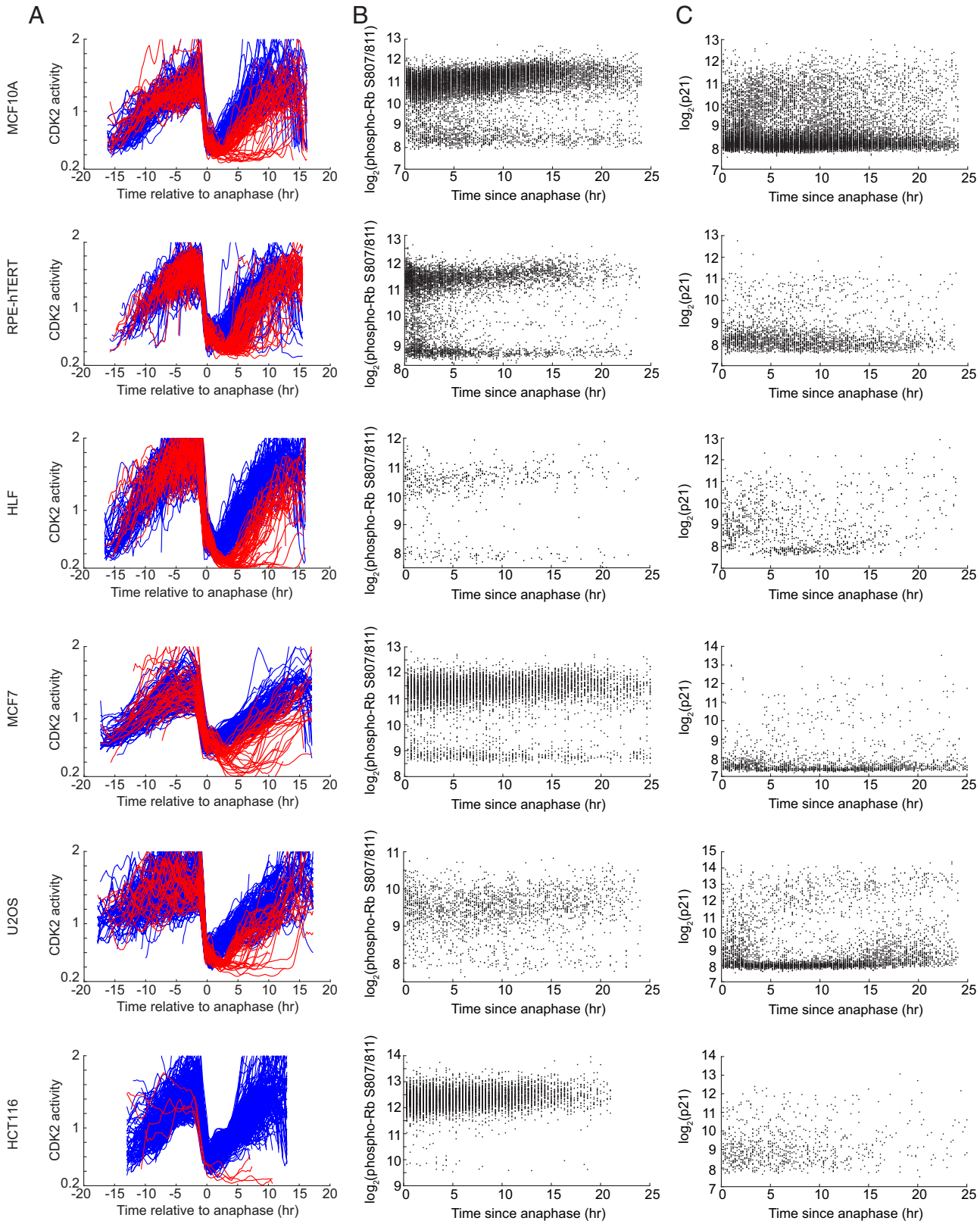

Fig. 2. Evidence for the generalizability of the bifurcation in CDK2 activity, Rb phosphorylation, and p21 expression. (*A*) Single-cell traces of CDK2 activity for CDK2^{inc} cells (blue) and CDK2^{low} cells (red). For clarity, 250 manually verified traces are plotted for each cell line of thousands analyzed; the numbers of CDK2^{inc} and CDK2^{low} traces plotted here are proportional to the fractions of each at the population level. CDK2^{low}: MCF10A, 26%; RPE-hTERT, 31%; HLF, 23%; MCF7, 18%; U2OS, 17%; and HCT116, 1%. (*B*) Single-cell measurement of phospho-Rb (S807/811) as a function of time-since-anaphase for all cells analyzed. Cells were imaged for 24 h, fixed, and stained for phospho-Rb, and the immunofluorescence image was registered to the final frame of the movie. MCF10A, n = 15,446 cells; RPE-hTERT, n = 11,936 cells; HLF, n = 547 cells; MCF7, n = 7,659 cells; U2OS, n = 5,348 cells; and HCT116, n = 8,157 cells. (*C*) Single-cell measurement of p21 as a function of time-since-anaphase as in *B*. MCF10A, n = 19,052 cells; RPE-hTERT, n = 2,809 cells; HLF, n = 1,019 cells; MCF7, n = 1,929 cells; U2OS, n = 4,958 cells; and HCT116, n = 825 cells.

CDK2^{low}, whereas MCF7 and U2OS cells were intermediate with 18 and 17% CDK2^{low}, respectively. HLF cells were comparable with these, with 23% of cells entering the CDK2^{low} state, whereas RPE-hTERT cells were the least likely to immediately enter another cell cycle, with 31% entering the CDK2^{low} state after mitosis under optimal growth conditions.

We next examined the phosphorylation state of Rb in these six cell types. Not only is Rb a canonical CDK2 substrate, but the phosphorylation status of this protein is considered an indicator of a cell's position relative to the Restriction Point (18, 24, 25). After 24 h of time-lapse imaging, we fixed and stained cells for phospho-Rb at Serine 807/811. Phospho-Rb is bimodally distributed (*SI Appendix*, Fig. S1), and we consider the high mode to represent hyperphosphorylated Rb as was done previously (14, 23, 26). Through image registration, we linked the immunofluorescence data to the time-lapse data to determine how long ago each cell underwent anaphase (Fig. 2*B* and *SI Appendix*, Fig. S1). Phospho-Rb staining already shows clear bimodality one frame after anaphase (12 or 20 min depending on cell type) in all six cell types examined, indicating that the proliferative subpopulation maintains hyperphosphorylation of Rb from one cycle to the next as has previously been shown for MCF10A (26). Strikingly, the fraction of cells with hyperphosphorylated Rb immediately after anaphase is similar to the fraction of the population born into the CDK2^{inc} state (*SI Appendix*, Fig. S1). We then repeated this experiment, staining for p21 after 24 h of time-lapse imaging. A weakly bimodal or long-tailed distribution of p21 abundance is apparent within the first frame after anaphase (Fig. 2*C* and *SI Appendix*, Fig. S1). Both the hypophosphorylated Rb state and the high p21 population decrease as time-since-anaphase increases, highlighting the transient nature of the CDK2^{low} state.

Previous work by this group and others has shown that in MCF10A, RPE-hTERT, and Hs68 primary human fibroblasts, high p21 levels in G0/G1 cells are associated with 53BP1 nuclear bodies, a marker of DNA lesions (20, 21). We therefore asked if this relationship was conserved in the cancer cell lines used here. As was previously shown with MCF10A and RPE-hTERT, we find that G0/G1 cells with 53BP1 nuclear bodies have higher p21 levels than G0/G1 cells without 53BP1 nuclear bodies (*SI Appendix*, Fig. S2). Thus, the three cancer cell lines tested here seem to face the CDK2^{inc} vs. CDK2^{low} decision in the same way as reported previously for nontransformed cells, although the fraction of cells born committed to each fate varies across cell lines.

p21 Up-Regulation and Rb Dephosphorylation Are Temporally Separated. Given that asynchronously cycling cells already show differential Rb phosphorylation and p21 levels immediately after mitosis, we next asked when exactly this bifurcation in Rb status and p21 expression occurs. To this end, we fixed and stained asynchronously cycling, wild-type MCF10A cells for the mitotic marker phospho-histone H3 (pHH3) and either phospho-Rb or p21 and measured these three signals by flow cytometry. p21 was up-regulated in 30% of pHH3+ cells, mirroring the fraction of cells born into the CDK2^{low} state (Fig. 3*A*, upper right quadrant). In contrast, there was no discrete hypophosphorylated Rb population among pHH3+ cells. We therefore asked whether this unexpected result could be explained by the facts that phosphorylation of histone H3 is lost before anaphase and that phosphorylation of Rb is lost in CDK2^{low} cells after anaphase.

To more carefully examine the timing of dephosphorylation of Rb, we repeated the experiment using immunofluorescence microscopy, computationally isolated cells at each phase of mitosis based on Hoechst staining, and then evaluated the levels of pHH3 and phospho-Rb in the resulting mock film strips. Histone H3 is dephosphorylated in late anaphase, in agreement with

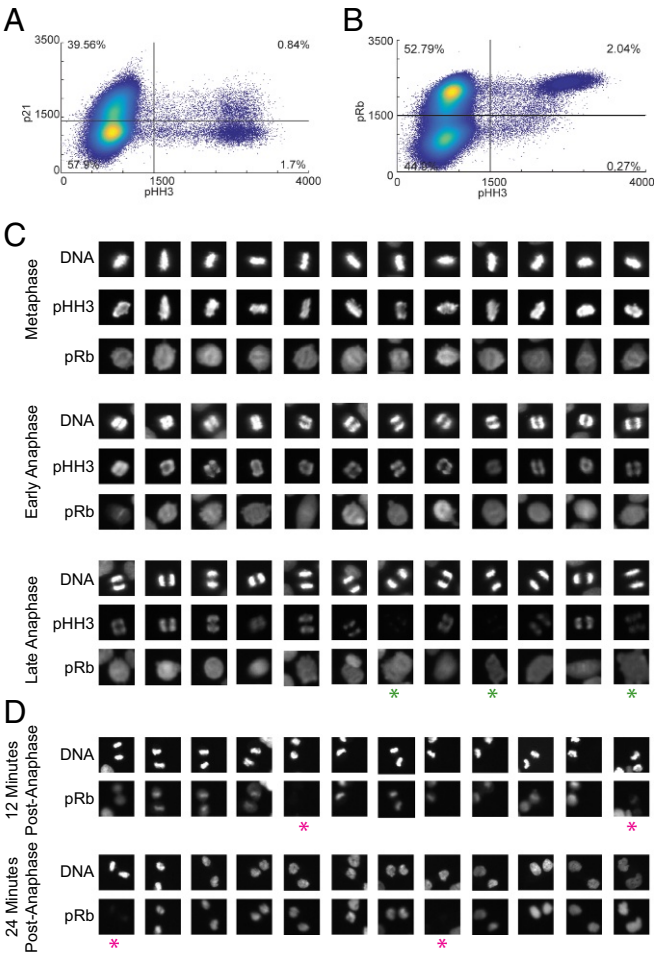

Fig. 3. A subset of cells matching the CDK2^{low} population up-regulates p21 before mitosis but does not dephosphorylate Rb until chromatin decondensation begins. (*A* and *B*) p21 signal (*A*) or phospho-Rb (pRb; S807/811) signal (*B*) as a function of pHH3 signal in asynchronously cycling MCF10A cells as measured by flow cytometry. Thirty-three percent of mitotic (pHH3+) cells have high p21 levels; 12% of mitotic cells have falling pRb, but there is no discrete hypophosphorylated Rb population (n = 10,000 cells). Gates were set according to the saddle point for p21 and pRb. (*C*) Asynchronously growing MCF10A cells were stained for pHH3, pRb (S807/811), and Hoechst. Mitotic cells were identified based on Hoechst staining and displayed as mock film strips. Anaphase cells are ordered based on distance between chromosomes. Histone H3 is dephosphorylated starting in late anaphase (green stars), whereas Rb is not dephosphorylated until after anaphase is complete and chromatin decondensation begins. (*D*) pRb (S807/811) in MCF10A cells from Fig. 2*B*. Shown are newly born cells fixed 12 min (*Upper*) or 24 min (*Lower*) after anaphase was detected. Cells are ordered based on chromatin decondensation and distance between sister cells. The numbers of cells with hyper- and hypophosphorylated Rb presented here are proportional to the total population. Green stars mark cells that are pHH3−; magenta stars mark cells with hypophosphorylated Rb.

previous literature (27–30), whereas Rb is not dephosphorylated until after late anaphase (Fig. 3 *C* and *D*), explaining why no discrete pHH3+/hypophosphorylated Rb population is detectable by flow cytometry. Synthesizing our flow cytometry, film strip, and time-lapse microscopy data (where we have immunofluorescence data for phospho-Rb beginning 12 min after anaphase), we conclude that Rb dephosphorylation in CDK2^{low} cells occurs in telophase after chromosome decondensation has started. The differential timing of p21 up-regulation in G2 and Rb dephosphorylation in telophase suggests that p21 up-regulation (by inhibiting CDK activity) causes entry into the CDK2^{low} state,

whereas Rb dephosphorylation (due to mitotic phosphatase activity and a dearth of CDK activity as CDK2^{low} cells exit mitosis) is a consequence.

p21 Up-Regulation Precedes Mitosis in Mother Cells Whose Daughters Enter the CDK2^{low} State After Mitosis. The similarity between the fraction of cells exiting the cell cycle after anaphase and the fraction of mitotic cells with high p21 prompted us to ask when exactly the up-regulation of p21 occurs. Given the importance of p21 in controlling the bifurcation in CDK2 activity (14, 20, 21, 31), we used CRISPR-Cas9 to engineer MCF10A that express mCitrine-tagged p21 from the endogenous *CDKN1A* locus (*SI Appendix*, Figs. S3 and S4). Although some studies have highlighted the potential for N-terminal acylation or ubiquitylation as a regulatory mechanism for p21 (32, 33), we targeted the N terminus of p21 because similarly tagged constructs have been shown to maintain functional p21 (14, 31). p21 tagged at the N terminus localizes normally, degrades similarly to wild-type p21, can still interact with CDK2, and does not dramatically alter cell cycle dynamics (*SI Appendix*, Fig. S4).

We also examined three other cell lines in which p21 is tagged at the C terminus with a fluorescent protein at the endogenous locus [RPE-hTERT (21), MCF7, and HCT116 (34)] or expressed from an inducible promoter at endogenous levels [U2OS (35)]. Each cell line was transduced with a fluorescently tagged H2B nuclear marker and the CDK2 sensor and then imaged for 24 h (Movies S2–S6). Cells from each population were classified according to CDK2 activity after anaphase: CDK2^{inc}, CDK2^{low}, and cells that emerge from the CDK2^{low} state 4–7 or 7–10 h after anaphase (CDK2$^{emerge4–7\ h}$ and CDK2$^{emerge7–10\ h}$, respectively). The single-cell CDK2 and p21 traces were then averaged within these four groups and aligned to the time of anaphase (Fig. 4 *A* and *B*).

Contrary to early models of cell cycle-dependent p21 expression (36, 37), we find that p21 up-regulation is not a general feature of G2. Instead, daughter cells that enter the CDK2^{inc} state after mitosis maintain low levels of p21 in the previous G2 and M, while daughter cells that enter the CDK2^{low} state after mitosis start up-regulating p21 5–10 h before anaphase, depending on the cell line (Fig. 4*B*). These CDK2^{low} daughter cells then continue to increase p21 levels after anaphase, sustaining the CDK2^{low} state. In contrast, CDK2^{emerge} cells that initially enter the CDK2^{low} state and then reenter the cell cycle show a decline in p21 levels around the time of cell cycle reentry.

p21 Degradation Is Initiated at the Restriction Point. To determine when CDK2^{emerge} cells down-regulate p21 relative to when they reactivate CDK2 and cross the Restriction Point, we aligned and averaged single-cell CDK2 activity traces from CDK2^{emerge} cells to the time of the rise in CDK2 activity (the Restriction Point) and monitored the levels of p21. While there is some cell-to-cell heterogeneity in the timing of p21 degradation relative to the timing of CDK2 activation (*SI Appendix*, Fig. S6), our analysis revealed that, on average, p21 continues to accumulate in newly born CDK2^{low} cells until the Restriction Point, at which point p21 levels fall dramatically (Fig. 4*C* and *SI Appendix*, Fig. S5). The near-simultaneous nature of rising CDK2 activity and falling p21 is consistent with the notion that CDK2 activity promotes the degradation of p21, an idea that has been predicted by analogy to p27 (38, 39) but cannot as of this writing be directly tested due to a lack of selective CDK2 inhibitors. To test instead the hypothesis that the degradation of p21 begins at the Restriction Point, we treated asynchronously cycling MCF10A cells with MLN4924, which inhibits Cullin-based E3 ligase complexes, and selected for analysis only CDK2$^{emerge4–7\ h}$ cells that received the drug 3–4 h after the Restriction Point (Fig. 4*D*). Whereas cells receiving vehicle continue to down-regulate p21 after crossing the Restriction Point, cells receiving MLN4924 rapidly reaccumulate p21. In contrast, p21 levels do not deviate from their increasing trajectory in CDK2^{low} cells on treatment with MLN4924 (Fig. 4*E*). We conclude that CDK2^{low} cells do not actively degrade p21 and that degradation of p21 begins coincident with the rise in CDK2 activity at the Restriction Point.

Discussion and Conclusions

A long-standing model of the cell cycle suggests that cells are born into a pre-Restriction Point state in which they are uncommitted to proliferation. For the first few hours after anaphase, cells are thought to integrate environmental signals to determine if they can cross the Restriction Point. After they cross this point, they are committed to one round of the cell cycle, and the resulting daughter cells are again born into an uncommitted pre-Restriction Point state. The groundbreaking studies that established this model relied predominately on cell cycle synchronization and bulk population analysis, which perturb the cell cycle and mask heterogeneity in cell behavior. The rise of single-cell analysis has challenged aspects of this model, suggesting instead that, in actively cycling cells, the uncommitted CDK2^{low} state is sampled only by a subset of cells (14) that experienced stress (20–23, 40) or blockade of MAPK signaling (14, 23, 26, 41) during the previous cell cycle.

In line with this recent trend, this study uses a combination of single-cell time-lapse imaging and fixed-cell analysis to show, across a number of primary, immortalized but not transformed, and cancerous cell types, that only a subset of cells in a population enters the uncommitted CDK2^{low} state after mitosis. Furthermore, independent of the CDK2 sensor, this heterogeneity is visible by immunofluorescence staining of Rb phosphorylation and p21, where a subset of cells exits mitosis with hyperphosphorylated Rb and low p21, while the remainder has hypophosphorylated Rb and high p21. The conclusion that a subset of cells is born committed to proliferation is further supported by the observation that, when subjected to serum withdrawal or acute Mek inhibition, CDK2^{inc} cells finish the current cell cycle, even if they are so perturbed in early G1 (14). Thus, immediately after anaphase, CDK2^{inc} cells are already in a post-Restriction Point state. In contrast, CDK2^{low} cells remain sensitive to serum withdrawal and Mek inhibition as long as they are in the CDK2^{low} state. These cells become insensitive to these perturbations after CDK2 activity rises and they cross the Restriction Point (14, 17). Our results, therefore, argue that only a subset of cells exits mitosis into a pre-Restriction Point state. Contrary to recent work (17), we find this can be true even for primary HLFs. Additionally, the similarity between the fraction of the population with hyperphosphorylated Rb and the fraction CDK2^{inc} suggests that the size of the proliferative subpopulation can be estimated from simple fixed cell immunofluorescence of phospho-Rb.

Several lines of evidence suggest that a cause of entry into the pre-Restriction Point CDK2^{low} state is high p21, including that p21$^{-/-}$ cells rarely enter the CDK2^{low} state and that acute overexpression of p21 in G2 is sufficient to send all cells into the CDK2^{low} state after mitosis (14, 20, 31). Here, we show that endogenous p21 begins to increase during G2 in mother cells whose daughters enter the CDK2^{low} state after mitosis, whereas mothers of CDK2^{inc} daughters have significantly less p21 both before and after anaphase. Notably, this pattern is not dependent on whether p21 is fused to a fluorescent protein at the N terminus (MCF10A, U2OS) or the C terminus (RPE-hTERT, MCF7, HCT116) or if the fluorescent p21 is expressed at endogenous levels off an inducible promoter (U2OS) or from the endogenous *CDKN1A* locus, suggesting the existence of both

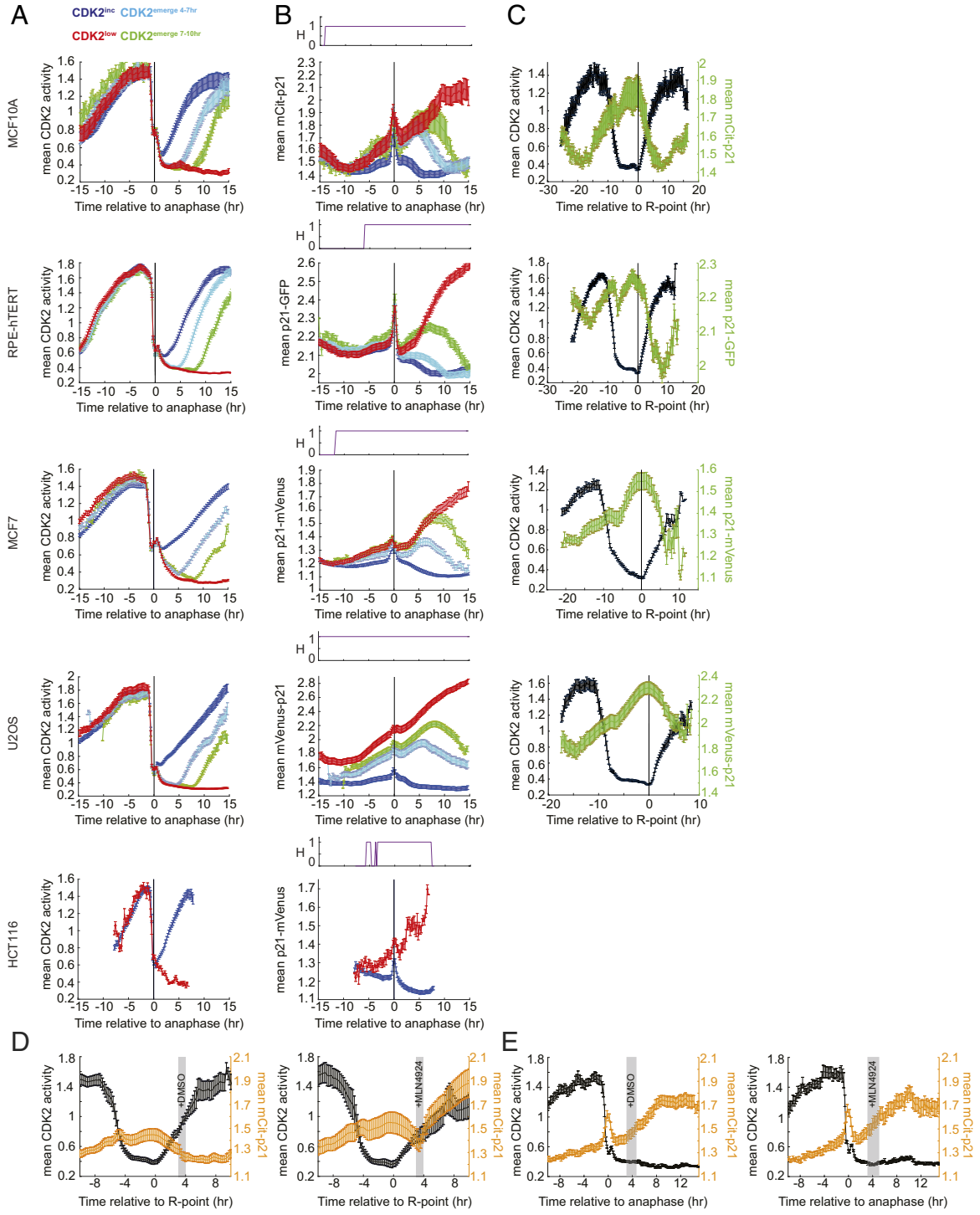

Fig. 4. p21 up-regulation precedes mitosis in mother cells whose daughters enter the CDK2^{low} state after mitosis, and p21 is degraded at the Restriction Point. (*A*–*C*) Cells expressing the CDK2 sensor and fluorescent p21 from the endogenous locus (with the exception of U2OS, which were induced to endogenous levels with doxycycline) were imaged for 24 h, tracked, classified according to CDK2 activity after anaphase, averaged, and aligned to either the time of anaphase (*A* and *B*) or the Restriction Point (*C*), which was defined as the time that CDK2 activity begins to rise. (*A*) CDK2 activity traces were classified as CDK2^{low} if the CDK2 activity dropped below the cutoff indicated in *Materials and Methods* and remained below this cutoff for the remainder of the imaging period. Traces were classified as CDK2$^{emerge\ 4–7\ h}$ or CDK2$^{emerge\ 7–10\ h}$ if the CDK2 activity dropped below the cutoff indicated in *Materials and Methods* and rose above this cutoff 4–7 or 7–10 h after anaphase, respectively; otherwise, traces were classified as CDK2^{inc}. A CDK2^{emerge} population does not exist for HCT116 cells because few cells enter the CDK2^{low} state. (*B*) Averaged p21 traces for the categories described in *A*. The purple line above each plot indicates the hypothesis testing result of a two-sample *t* test with *P* value < 0.05, comparing p21 in CDK2^{inc} with CDK2^{low} cells at each time point. (*C*) Averaged p21 and CDK2 activity traces for CDK2$^{emerge7–10\ h}$ cells aligned to the Restriction Point. (*D*) Averaged p21 (orange) and CDK2 activity (black) traces from MCF10A CDK2$^{emerge4–7\ h}$ cells aligned to the Restriction Point. Only those cells receiving DMSO (*Left*) or 1.4 μM MLN4924 (*Right*) 3–4 h (gray shading) after CDK2 had begun to rise are included. (*E*) Averaged p21 (orange) and CDK2 activity (black) traces from MCF10A CDK2^{low} cells that received DMSO (*Left*) or 1.4 μM MLN4924 (*Right*) 3–5 h (gray shading) after anaphase. Error bars represent SEM. Data presented here are representative of two biological replicates. Cell counts for each group can be found in *SI Appendix*. mCit-p21, mCitrine-tagged p21 from the endogenous CDKN1A locus. p21 axis units are in log(10).

p53 transcription-dependent and p53 transcription-independent regulation of p21 in the proliferation–quiescence decision. The observation that p21 dynamics are independent of whether p21 expression is off the endogenous promoter or via a doxycycline-inducible promoter suggests that posttranslational modifications play an essential role in regulating abundance of this protein and by extension, cell fate. We note that tagged p21 seems to be more highly expressed than the wild type (*SI Appendix*, Fig. S4), possibly due to the loss of N terminus-driven degradation (32, 33). Nevertheless, both N- and C-terminal tagged p21 dynamics are similar. Our results reveal that the graded input of p21 levels in G2/M is converted to a binary output, resulting in proliferative $CDK2^{inc}$ and transiently quiescent $CDK2^{low}$ daughter cells after mitosis.

If replication stress at the end of S phase leads to incompletely replicated genomic loci (20, 21, 42, 43), why does this not trigger a G2/M checkpoint? Do cells simply not detect the problem? Our data suggest that, in response to low levels of endogenous replication stress, a cellular warning signal is indeed triggered in G2 in the form of up-regulation of the CDK inhibitor p21 but that the levels of p21 attained before mitosis are insufficient to block progression through mitosis due to the very high levels of CDK2 and CDK1 activity in cells during G2 and M. Cells therefore proceed through mitosis and then arrest at the start of the new cell cycle when CDK activity is low again and when p21 levels are sufficient to block CDK-mediated cell cycle progression. In general, arrest of daughter cells in a $CDK2^{low}$ state after mitosis is likely easier to sustain long term than a G2/M arrest, although recent work in *Drosophila* has suggested the possibility of a G2 quiescence, at least in stem cells (44). Thus, our data suggest that G2 phase in mother cells represents a window, referred to previously as R_1 (14) or as the maternal window of signal integration here, where cells sense both mitogens and stress and initiate a response, which is then converted into a bifurcation in CDK2 activity after mitosis. For $CDK2^{inc}$ cells committed to proliferation, this window is closed by the start of the new cell cycle, whereas the window of signal integration remains open for $CDK2^{low}$ cells, allowing them to continue integrating mitogen and stress signals until they cross the Restriction Point and commit to a new cell cycle.

These $p21^{high}/CDK2^{low}$ cells can reenter the cell cycle by degrading p21 at the Restriction Point. Thus, p21 degradation reflects the decision to resume proliferation from the $CDK2^{low}$ state. This result is consistent with recent observations that p21 degradation can begin before S phase (21, 34) and contrasts with other models of p21 degradation, which hold that p21 degradation begins at the start of S phase (35–37). While the presence of the proliferating cell nuclear antigen (PCNA)-interacting protein (PIP) degron in p21 (35) and the potential for PCNA-dependent degradation of this protein by $CRL4^{Cdt2}$ (45) are important for active degradation of p21 in S phase, it is possible that PCNA-dependent degradation is a redundant system to guarantee that p21 will not be present at high enough levels to impede S-phase progression (31, 42) and that a PCNA-independent degradation mechanism initiates p21 destruction at the Restriction Point, several hours before the start of S phase. The relationship between p21 degradation and passage through the Restriction Point further suggests an intimate connection between the two, wherein the Restriction Point is not only sensitive to mitogens but also to DNA damage via p21. Whereas the role of mitogens in Restriction Point control has been extensively studied, when and how cells down-regulate p21 to promote passage through the Restriction Point is an open area of investigation.

Why does the fraction of cells entering the $CDK2^{low}$ state vary from one cell line to the next? This study and earlier studies have focused on the roles that DNA damage and endogenous p21 play in the proliferation–quiescence decision (20, 21). If endogenous DNA damage arises in S phase, any variation in DNA replication error rates between cell lines will tune the fraction of the population exiting the cell cycle after mitosis. Furthermore, recent work has suggested that both DNA repair efficiency and basal ataxia telangiectasia mutated/ataxia telangiectasia and Rad3-related protein (ATM/ATR) activity inform p53 dynamics (46); given that p53 is the main transcription factor of p21 (47), how the interplay between these factors influences p53 dynamics may in turn inform the fraction of a population that exits the cell cycle after anaphase. Other molecules may also play a role in regulating the proliferation–quiescence decision, such as cyclins D and E (15, 48), p27, p57, Wee1, Cdc25 (49, 50), PP2A (19), and USP11 (51). Alternate routes out of the cell cycle may explain the fraction of transits through the $CDK2^{low}$ state that are not explained by inherited DNA damage from mother cells (20). The up- or down-regulation of any one of these proteins in a given cell line would help determine the fraction of cells entering the $CDK2^{low}$ state after mitosis. Indeed, HCT116 cells may avoid cell-cycle exit via the overexpression of low-molecular weight cyclin E (52). Furthermore, the availability of mitogens is a key factor—under cell culture conditions with saturating growth factors as used here, cells are likely to achieve their proliferative potential. In this regime, the alternative cell cycle model depicted in Fig. 1*B* is clearly evident, with a majority of cells committing immediately to another cell cycle, and therefore, cells will be limited primarily by stress. Conversely, under more physiological conditions, in which mitogens are limiting, proliferation will be constrained by both mitogens and stress, and a higher fraction of cells will enter the $CDK2^{low}$ state after mitosis.

Our model is predicated on cells having intact Rb and p53; cell lines without functional p53 may not be able to use p21 to enter the $CDK2^{low}$ state. Unless these cells have alternative means of suppressing CDK2 activity, we expect cells lacking p53 to cycle continuously, such as was shown previously in cells where p21 or p53 was depleted or eliminated (14, 20, 21).

Our data show that the classic model of the cell cycle, in which cells are born into a pre-Restriction Point state with hypophosphorylated Rb, is not universally applicable, and in fact, it is not well-suited to any of the cell types examined here, including primary HLFs. Instead, all six cell types that we examined are split such that some cells reset to a pre-Restriction Point state, while others (the majority in the case of the six cell types examined here) are born without ever having "uncrossed" the Restriction Point and are thus immediately committed to another cell cycle. Put another way, healthy cells in optimal mitogenic conditions do not reset to a pre-Restriction point state and therefore continue cycling.

Although all cell types examined here have the Restriction Point machinery intact, only $CDK2^{low}$ cells reset to a pre-Restriction Point state. In other words, whereas all or most cells seem to have a maternal window in which they integrate mitogenic and stress signaling, only daughter cells entering the $CDK2^{low}$ state experience the canonical Restriction Point in the daughter cell cycle. This then implies that the Restriction Point must be located at the end of the $CDK2^{low}$ period. Thus, rather than occurring specifically 3–4 h after mitosis, the Restriction Point is better conceptualized as the variable time point at which the cell decides to reenter the cell cycle, degrade p21, and build up CDK2 activity. Positioning the Restriction Point outside the cell cycle as in Fig. 1*B*, where it is only ever reset in cells that enter the $CDK2^{low}$ state, also explains the dramatic heterogeneity in cell cycle duration across a given population. Residence time in the pre-Restriction Point $CDK2^{low}$ state is variable, and cell cycle duration varies according to the length of time that it takes for those cells to cross the Restriction Point. In summary, our

data support the alternative model in Fig. 1*B*, where the decision to proliferate is informed by events occurring at the end of the previous cell cycle and only a subset of cells resets to a pre-Restriction Point state after mitosis.

Materials and Methods

Cell Culture and Maintenance. MCF10A (ATCC CRL-10317) were maintained in DMEM/F12 supplemented with 5% horse serum, 100 ng/mL cholera toxin, 20 ng/mL EGF, 10 μg/mL insulin, 0.5 μg/mL hydrocortisone, and 100 μg/mL each penicillin and streptomycin. RPE-hTERT [ATCC CRL-4000 and those tagged with p21-GFP (21)] were maintained in DMEM/F12 supplemented with 10% FBS, 1× Glutamax, and 100 μg/mL each penicillin and streptomycin. MCF7 were maintained in RPMI supplemented with 10% FBS, 1× Glutamax, and 100 μg/mL each penicillin and streptomycin. U2OS and HCT116 were maintained in McCoy's 5A supplemented with 10% FBS and 100 μg/mL each penicillin and streptomycin. Primary fetal HLFs (507-75f; Cell Applications) were maintained in Human Lung Fibroblast Growth Medium (516-500; Cell Applications), in contrast with the growth conditions used in ref. 17. For live-cell imaging, each cell line was maintained in a phenol red-free version of their growth media; HLFs were imaged in Human Lung Fibroblast Growth Medium. U2OS were seeded with 10 ng/μL doxycycline to induce endogenous-level expression of fluorescent p21 (35) for at least 24 h before imaging. All cell lines were grown in a humidified incubator (5% CO_2, 37 °C). MCF7 and HCT116 cells with p21 tagged at the endogenous locus were provided by the laboratory of Galit Lahav, Department of Systems Biology, Harvard Medical School, Boston (34). RPE-hTERT with p21 tagged at the endogenous locus was provided by the laboratory of Chris Bakal, Division of Cancer Biology, Institute of Cancer Research, London (21). U2OS cells with inducible p21 were provided by the laboratory of Jeanette Cook, Department of Biochemistry and Biophysics, University of North Carolina at Chapel Hill, Chapel Hill, NC (35).

Cell Line Generation. Low-passage wild-type MCF10A were transfected with a plasmid encoding CRISPR-Cas9, single-guide (sg)RNA targeting the 5′ end of CDKN1A, and a repair template encoding the mCitrine gene; the left and right homology arms extended for 1,000 bp upstream and downstream of the CDKN1A start codon. The sgRNA sequence used was GCGCCATGTCAGAACCGGCTGGG. Cells were transfected in antibiotic-free medium and supplemented with 1 μM SCR7, an inhibitor of nonhomologous end joining (SML1546; Sigma). Cells were allowed to recover and expand before the YFP-positive cells were isolated via FACS. Clonal lines were then expanded and validated by PCR, genomic DNA sequencing, immunofluorescence, and Western blotting (*SI Appendix*, Figs. S3 and S4).

Cells used for time-lapse live-cell microscopy were transduced with a nuclear marker [H2B-mTurquoise or H2B-miFP (53)] and the CDK2 sensor DHB (14) using established lentivirus protocols, and double-positive cells were sorted by FACS. CDK2 activity was read out as the cytoplasmic to nuclear ratio of the DHB sensor. Primary HLFs were transduced with H2B-mTurquoise and DHB-mCherry at passage 2 and were imaged at passage 5.

Flow Cytometry. MCF10A were harvested through trypsinization and resuspended in DMEM/F12 supplemented with 20% horse serum. The cell pellet was washed twice with PBS, and the cells were fixed and permeabilized with ice-cold methanol at −20 °C. The population was then split, and cells were stained for pHH3 (CST 9706) and either p21 (CST 2947S) or phospho-Rb (S807/811; CST 8516S) followed by secondary antibody staining. Fluorescence intensities for each signal were read on a MoFlo Cytomation and analyzed using custom MATLAB scripts.

Imaging and Image Processing. Time-lapse imaging, immunofluorescence, image processing, and classification of populations were conducted as previously described (15, 20). Both fixed and time-lapse microscopy images were processed as previously described (26). The tracking code is available for download here: https://github.com/scappell/Cell_tracking. Additional detail is available in *SI Appendix*.

ACKNOWLEDGMENTS. We thank Galit Lahav, Jean Cook, and Chris Bakal for cell lines with fluorescently tagged p21 and the members of the laboratory of S.L.S. for general help, especially Chen Yang for H2B-miFP lentivirus. This work was supported by NIH Training Grant T32 GM 8759-16 (to J.M.), NIH Instrumentation Grant S10OD021601, NIH K22 Early-Career Investigator Award 1K22CA188144-01, a Boettcher Webb-Waring Early-Career Investigator Award, a Kimmel Scholar Award SKF16-126, a Pew-Stewart Scholar for Cancer Research Award, a Searle Scholar Award SSP-2016-1533, and a Beckman Young Investigator Award (to S.L.S.).

1. Hanahan D, Weinberg R (2011) Hallmarks of cancer: The next generation. *Cell* 144:646–674.
2. Pardee AB (1974) A restriction point for control of normal animal cell proliferation. *Proc Natl Acad Sci USA* 71:1286–1290.
3. Jones SM, Kazlauskas A (2001) Growth-factor-dependent mitogenesis requires two distinct phases of signalling. *Nat Cell Biol* 3:165–172.
4. Zwang Y, et al. (2011) Two phases of mitogenic signaling unveil roles for p53 and EGR1 in elimination of inconsistent growth signals. *Mol Cell* 42:524–535.
5. Zetterberg A, Larsson O (1985) Kinetic analysis of regulatory events in G1 leading to proliferation or quiescence of Swiss 3t3 cells. *Proc Natl Acad Sci USA* 82:5365–5369.
6. Baldin V, Lukas J, Marcote MJ, Pagano M, Draetta G (1993) Cyclin D1 is a nuclear protein required for cell cycle progression in G1. *Genes Dev* 7:812–821.
7. Ezhevsky SA, et al. (1997) Hypo-phosphorylation of the retinoblastoma protein (pRb) by cyclin D: Cdk4/6 complexes results in active pRb. *Proc Natl Acad Sci USA* 94:10699–10704.
8. Hinds PW, et al. (1992) Regulation of retinoblastoma protein functions by ectopic expression of human cyclins. *Cell* 70:993–1006.
9. Zarkowska T, Mittnacht S (1997) Differential phosphorylation of the retinoblastoma protein by G1/S cyclin-dependent kinases. *J Biol Chem* 272:12738–12746.
10. Ludlow JW, Glendening CL, Livingston DM, DeCarprio JA (1993) Specific enzymatic dephosphorylation of the retinoblastoma protein. *Mol Cell Biol* 13:367–372.
11. Yao G, Lee TJ, Mori S, Nevins JR, You L (2008) A bistable Rb-E2f switch underlies the restriction point. *Nat Cell Biol* 10:476–482.
12. Akiyama T, Ohuchi T, Sumida S, Matsumoto K, Toyoshima K (1992) Phosphorylation of the retinoblastoma protein by cdk2. *Proc Natl Acad Sci USA* 89:7900–7904.
13. Weinberg RA (2013) *The Biology of Cancer* (Garland Science, New York), 2nd Ed.
14. Spencer SL, et al. (2013) The proliferation-quiescence decision is controlled by a bifurcation in CDK2 activity at mitotic exit. *Cell* 155:369–383.
15. Gookin S, et al. (2017) A map of protein dynamics during cell-cycle progression and cell-cycle exit. *PLoS Biol* 15:e2003268.
16. Miller I, et al. (2018) Ki67 is a graded rather than a binary marker of proliferation vs. quiescence. *Cell Rep* 24:1105–1112.
17. Schwarz C, et al. (2018) A Precise Cdk activity threshold determines passage through the restriction point. *Mol Cell* 69:253–264.e5.
18. Weinberg RA (1995) The retinoblastoma protein and cell cycle control. *Cell* 81:323–330.
19. Naetar N, et al. (2014) PP2a-mediated regulation of Ras signaling in G2 is essential for stable quiescence and normal G1 length. *Mol Cell* 54:932–945.
20. Arora M, Moser J, Phadke H, Basha AA, Spencer SL (2017) Endogenous replication stress in mother cells leads to quiescence of daughter cells. *Cell Rep* 19:1351–1364.
21. Barr AR, et al. (2017) DNA damage during S-phase mediates the proliferation-quiescence decision in the subsequent G1 via p21 expression. *Nat Commun* 8:14728.
22. Lezaja A, Altmeyer M (2018) Inherited DNA lesions determine G1 duration in the next cell cycle. *Cell Cycle* 17:24–32.
23. Yang HW, Chung M, Kudo T, Meyer T (2017) Competing memories of mitogen and p53 signalling control cell-cycle entry. *Nature* 549:404–408.
24. Blagosklonny MV, Pardee AB (2013) *The Restriction Point of the Cell Cycle* (Landes Bioscience, Austin, TX).
25. Lundberg AS, Weinberg RA (1999) Control of the cell cycle and apoptosis. *Eur J Cancer* 35:1886–1894.
26. Cappell SD, Chung M, Jaimovich A, Spencer SL, Meyer T (2016) Irreversible APCCdh1 inactivation underlies the point of no return for cell-cycle entry. *Cell* 166:167–180.
27. Hendzel MJ, et al. (1997) Mitosis-specific phosphorylation of histone H3 initiates primarily within pericentromeric heterochromatin during G2 and spreads in an ordered fashion coincident with mitotic chromosome condensation. *Chromosoma* 106:348–360.
28. Hooser AV, Goodrich DW, Allis CD, Brinkley BR, Mancini MA (1998) Histone H3 phosphorylation is required for the initiation, but not maintenance, of mammalian chromosome condensation. *J Cell Sci* 111:3497–3506.
29. Hans F, Dimitrov S (2001) Histone H3 phosphorylation and cell division. *Oncogene* 20:3021–3027.
30. Sauvé DM, Anderson HJ, Ray JM, James WM, Roberge M (1999) Phosphorylation-induced rearrangement of the histone H3 NH2-terminal domain during mitotic chromosome condensation. *J Cell Biol* 145:225–235.
31. Overton KW, Spencer SL, Noderer WL, Meyer T, Wang CL (2014) Basal p21 controls population heterogeneity in cycling and quiescent cell cycle states. *Proc Natl Acad Sci USA* 111:E4386–E4393.
32. Chen X, et al. (2004) N-acetylation and ubiquitin-independent proteasomal degradation of p21cip1. *Mol Cell* 16:839–847.
33. Bloom J, Amador V, Bartolini F, DeMartino G, Pagano M (2003) Proteasome-mediated degradation of p21 via N-terminal ubiquitinylation. *Cell* 115:71–82.
34. Stewart-Ornstein J, Lahav G (2016) Dynamics of CDKN1a in single cells defined by an endogenous fluorescent tagging toolkit. *Cell Rep* 14:1800–1811.
35. Coleman KE, et al. (2015) Sequential replication-coupled destruction at G1/S ensures genome stability. *Genes Dev* 29:1734–1746.
36. Dulić V, Stein GH, Far DF, Reed SI (1998) Nuclear accumulation of p21cip1 at the onset of mitosis: A role at the G2/M-phase transition. *Mol Cell Biol* 18:546–557.

37. Li Y, Jenkins CW, Nichols MA, Xiong Y (1994) Cell cycle expression and p53 regulation of the cyclin-dependent kinase inhibitor p21. *Oncogene* 9:2261–2268.
38. Nguyen H, Gitig DM, Koff A (1999) Cell-free degradation of p27kip1, a G1 cyclin-dependent kinase inhibitor, is dependent on CDK2 activity and the proteasome. *Mol Cell Biol* 19:1190–1201.
39. Zhu H, Nie L, Maki CG (2005) Cdk2-dependent inhibition of p21 stability via a C-terminal cyclin-binding motif. *J Biol Chem* 280:29282–29288.
40. Heldt FS, Barr AR, Cooper S, Bakal C, Novák B (2018) A comprehensive model for the proliferation–quiescence decision in response to endogenous DNA damage in human cells. *Proc Natl Acad Sci USA* 115:2532–2537.
41. Hitomi M, Stacey DW (1999) Cellular Ras and cyclin D1 are required during different cell cycle periods in cycling NIH 3t3 cells. *Mol Cell Biol* 19:4623–4632.
42. Harrigan JA, et al. (2011) Replication stress induces 53bp1-containing OPT domains in G1 cells. *J Cell Biol* 193:97–108.
43. Lukas C, et al. (2011) 53bp1 nuclear bodies form around DNA lesions generated by mitotic transmission of chromosomes under replication stress. *Nat Cell Biol* 13:243–253.
44. Otsuki L, Brand AH (2018) Cell cycle heterogeneity directs the timing of neural stem cell activation from quiescence. *Science* 360:99–102.
45. Abbas T, et al. (2008) PCNA-dependent regulation of p21 ubiquitylation and degradation via the CRL4cdt2 ubiquitin ligase complex. *Genes Dev* 22:2496–2506.
46. Stewart-Ornstein J, Lahav G (2017) p53 dynamics in response to DNA damage vary across cell lines and are shaped by efficiency of DNA repair and activity of the kinase ATM. *Sci Signal* 10:eaah6671.
47. El-Deiry WS, et al. (1993) WAF1, a potential mediator of p53 tumor suppression. *Cell* 75:817–825.
48. Hitomi M, Stacey DW (1999) Cyclin D1 production in cycling cells depends on Ras in a cell-cycle-specific manner. *Curr Biol* 9:1075–1784.
49. Donzelli M, Draetta GF (2003) Regulating mammalian checkpoints through Cdc25 inactivation. *EMBO Rep* 4:671–677.
50. Besson A, Dowdy SF, Roberts JM (2008) CDK inhibitors: Cell cycle regulators and beyond. *Dev Cell* 14:159–169.
51. Deng T, et al. (2018) Deubiquitylation and stabilization of p21 by USP11 is critical for cell-cycle progression and DNA damage responses. *Proc Natl Acad Sci USA* 115:4678–4683.
52. Vijayaraghavan S, et al. (2017) CDK4/6 and autophagy inhibitors synergistically induce senescence in Rb positive cytoplasmic cyclin E negative cancers. *Nat Commun* 8:15916.
53. Yu D, et al. (2015) A naturally monomeric infrared fluorescent protein for protein labeling in vivo. *Nat Methods* 12:763–765.